5.3 EVENT 3: ORBIT 790 (TYPICAL CHARGING, SUNSET CASE)

Overview data, 92.12.05, Prince Albert

Orbit 790 is famous in the Freja scientific community, since a well developed auroral substorm passed during this orbit, and several papers have been written about this substorm. However, no-one have addressed the charging event that seems to exist in the middle of the auroral activity and transverse ion heating. Figure 5.3.1 display the overview particle data. Between 0233:00 UT and 0243:00 UT a large auroral disturbance occurs with large fluxes of high energy electrons as measured by both the TESP instrument (panel 7) and the MATE instrument (panel 5). The ion population is uplifted in energy in the time interval 0234:00 - 0239:00 UT. Most of this particular time interval occurs during sunlight conditions (panel 4), and only the later part of the event is in eclipse. The eclipse is, of course, more gradual than the sharp time indicated in panel 4, and the whole uplifted ion event can be considered to occur during terminator conditions with a more smooth transition from sunlight to darkness as more and more of the Earth's atmosphere inhibit the solar radiation. The two Freja photometers were unfortunately not available during this event. The first part of the auroral event between 0233:00 - 0236:00 UT is most probably due to transverse ion heating, since no dropout exist in the LP current during these times. The later part is presented in more detail in Figure 5.3.2 and 5.3.3.

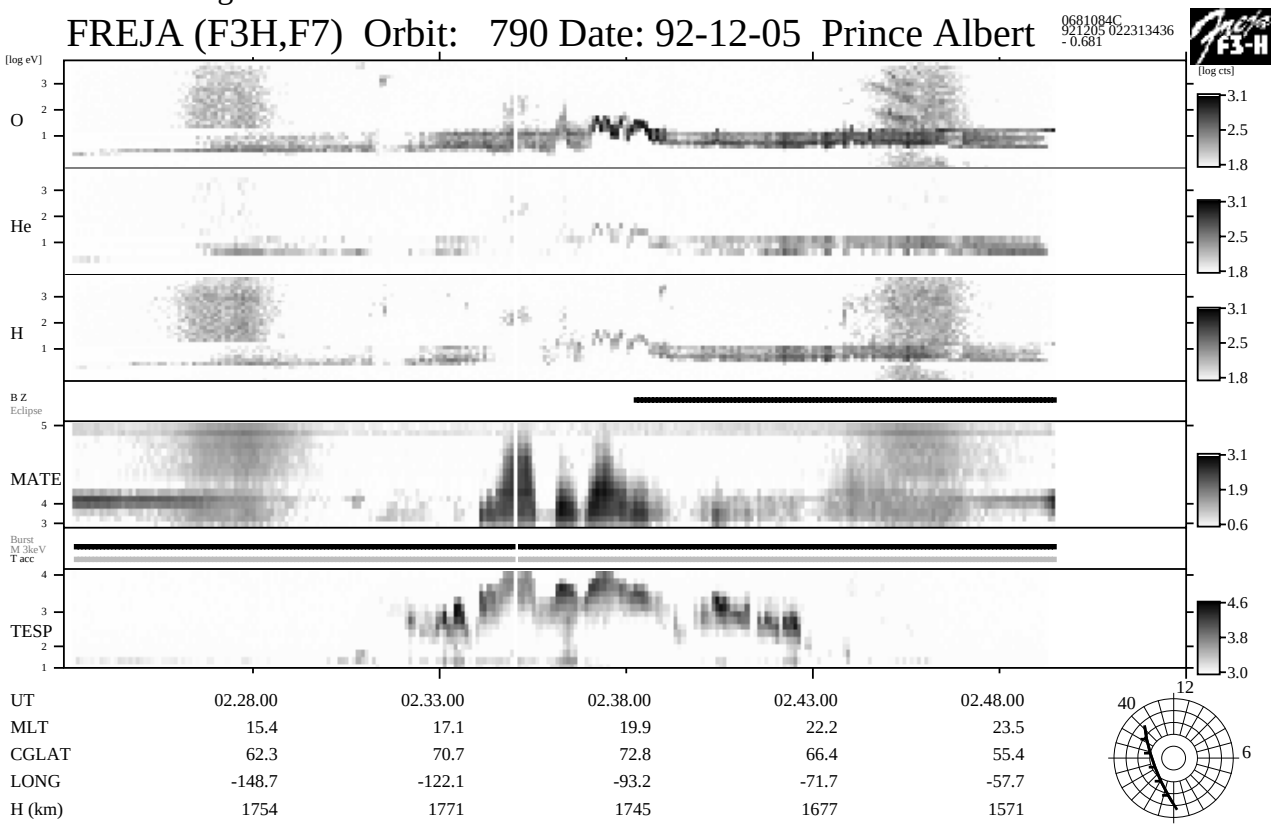

Figure 5.3.1: Overview particle data from orbit 790. Both MATE (panel 5) and TESP (panel 7) electron data existed when a full scale auroral substorm passed. A charging event occurred during this substorm around 0238:00 UT near the terminator (as seen in panel 4).

The estimated density from the HF narrow-band emissions (Figure 5.3.3, panel 1) is rather constant for the whole displayed interval and attains values close to 1.2-2.8·10^8 m^{-3}, while the CYLP current (panel 5) occasionally drops to very low values. Spacecraft charging is therefore suggested during those current drops. The ions are uplifted in energy to almost 100 eV (Figure 5.3.2, panels 1-3) during the CYLP current dropouts, and enhanced fluxes of high energy electrons (panels 5 and 7) correlates well in both flux intensity and maximum energy attained for these periods. We interpret these results that the electron flux and peak energy are major factors determining the charging level for a given plasma density.

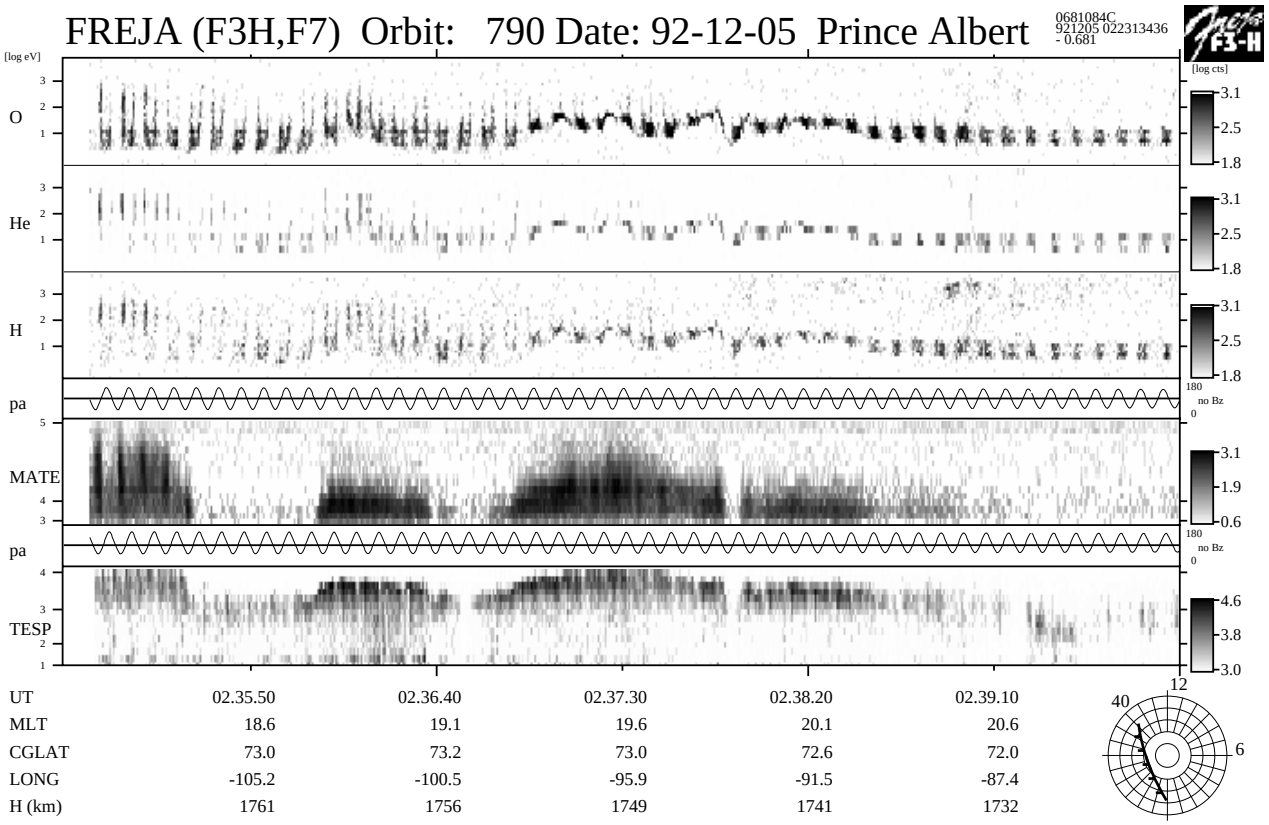

Figure 5.3.2: An enlargement of the data in Figure 5.3.1 around the charging period. Transverse ion heating related to the auroral substorm can be detected before 0237:00 UT.

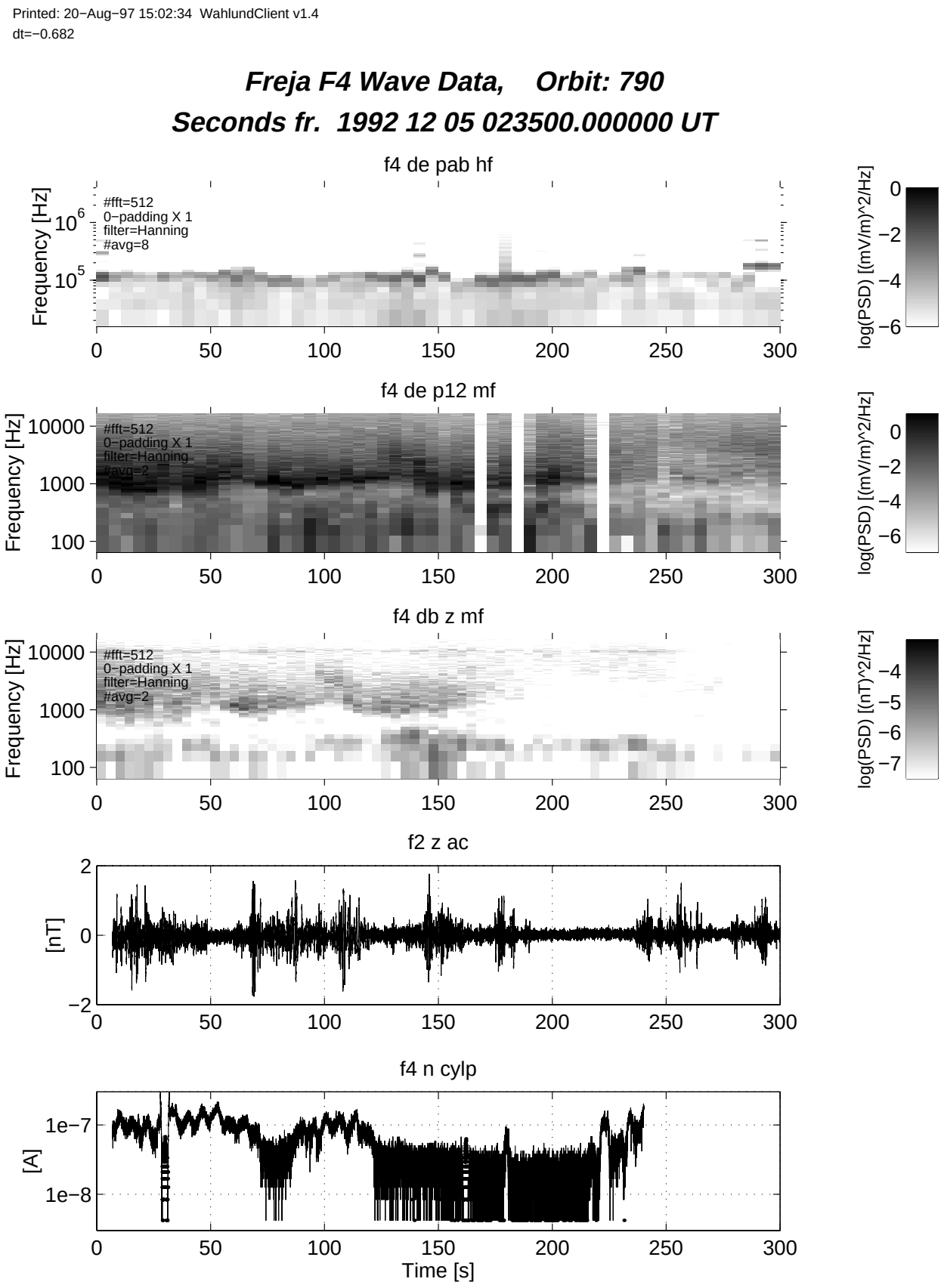

Figure 5.3.3: Narrow-band Langmuir emissions (panel 1) indicate an almost constant plasma density during the charging event. The periods of charging is inferred from the sudden drops in the sampled LP current near +80 s and around 170 s.

Detailed Distributions Around 0237:30 UT:

A series of TESP and MATE particle flux spectra are presented in Figures 5.3.4a - 5.3.4c and 5.3.5a - 5.3.5d respectively, which together covers the time period 0236:40 - 0238:10 UT. Note how these spectra evolve with time when the charging event starts, reaches its maximum, and then relax. The maximum of the inverted-V peak reaches large energies up to 10 keV during maximum charging (Figure 5.3.4b, all panels; Figure 5.3.5b, all panels; Figure 5.3.5c, panels 3 and 4), where also the largest electron fluxes at these highest energies of a few keV occurs. The precipitating electron fluxes are close to isotropic and belongs to an auroral inverted-V event. Thus, during the charging event the maximum flux of energetic electrons at the peak moves above the crossover energies of ITOC (2.5-3 keV) and the thermal blanket (just below 4 keV). This suggests that the flux of the emitted secondary electrons cannot longer balance the incident energetic electron flux, and in this way cause the observed negative charging. Also, the flux levels in the high energy tail up to 60 keV increases with about an order of magnitude, which further contribute to the excess negative charge accumulation.

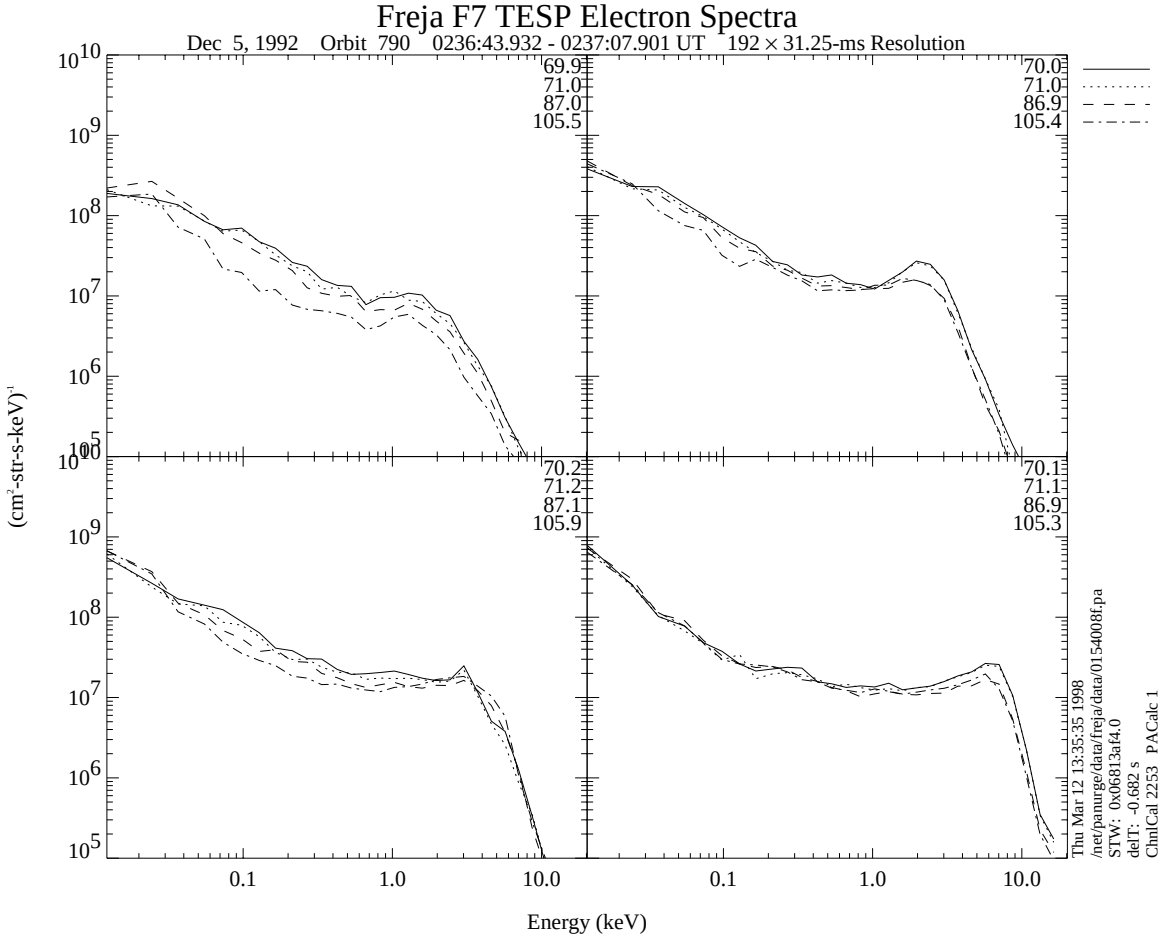

Figure 5.3.4a: The following three Figures with TESP data and four Figures with MATE data show the evolution of the electron spectra during the charging event. For the TESP measurements the charging start evolve in panels 2-3, to continue through Figure 5.3.4b, and start decline in panel 3-4 in Figure 5.3.4c. As soon as almost isotropic inverted-V peak reach above about 5 keV charging appears. Similarly, for the MATE data (Figure 5.3.5a-d) the charging event start in Figure 5.3.5b (panel 1) where the inverted-V peak reach 10 keV and continue to rise in energy (and flux) to panel 2-3 in Figure 5.3.5c, where after it declines in Figure 5.3.5d.

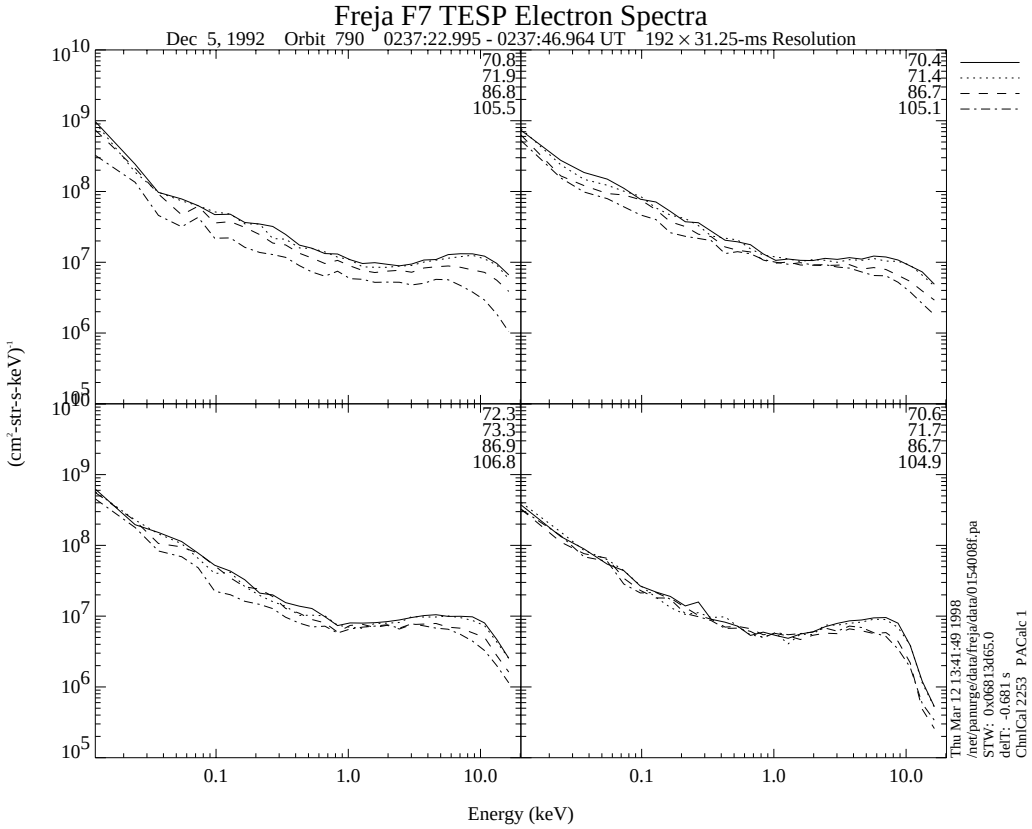

Figure 5.3.4b: See Figure 5.3.4a.

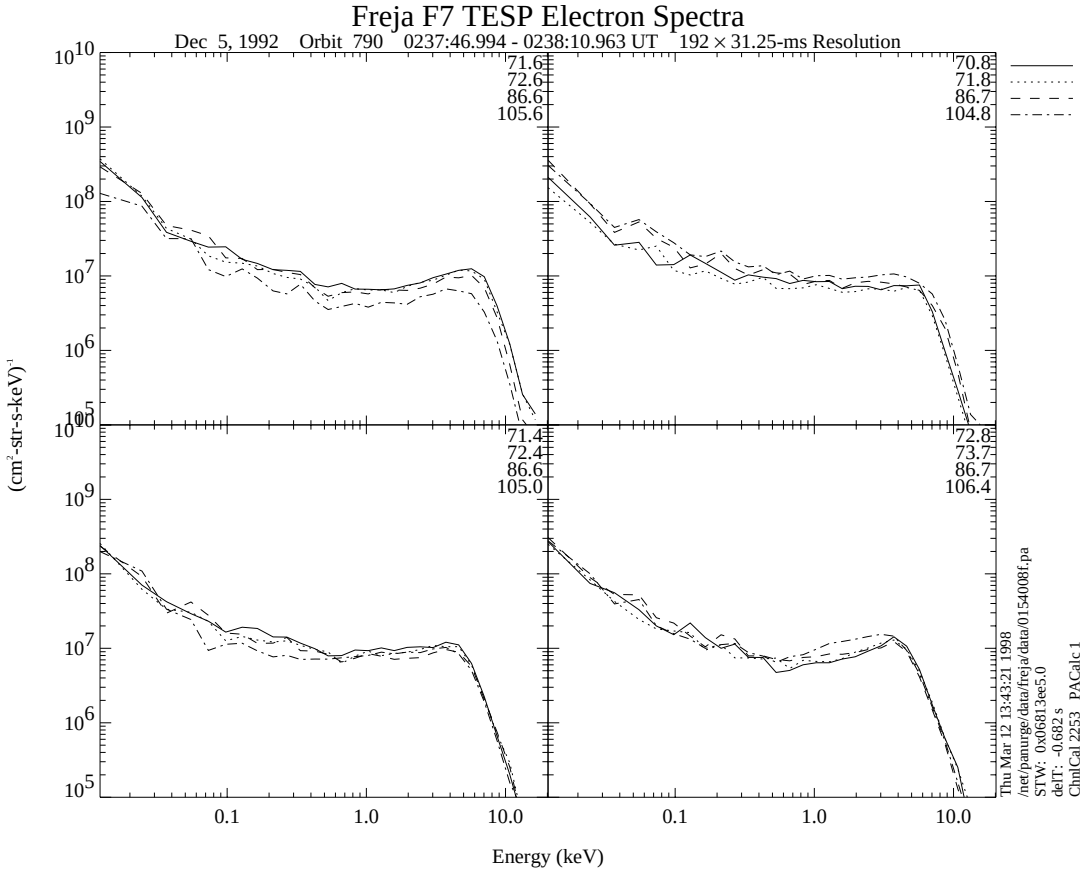

Figure 5.3.4c: See Figure 5.3.4a.

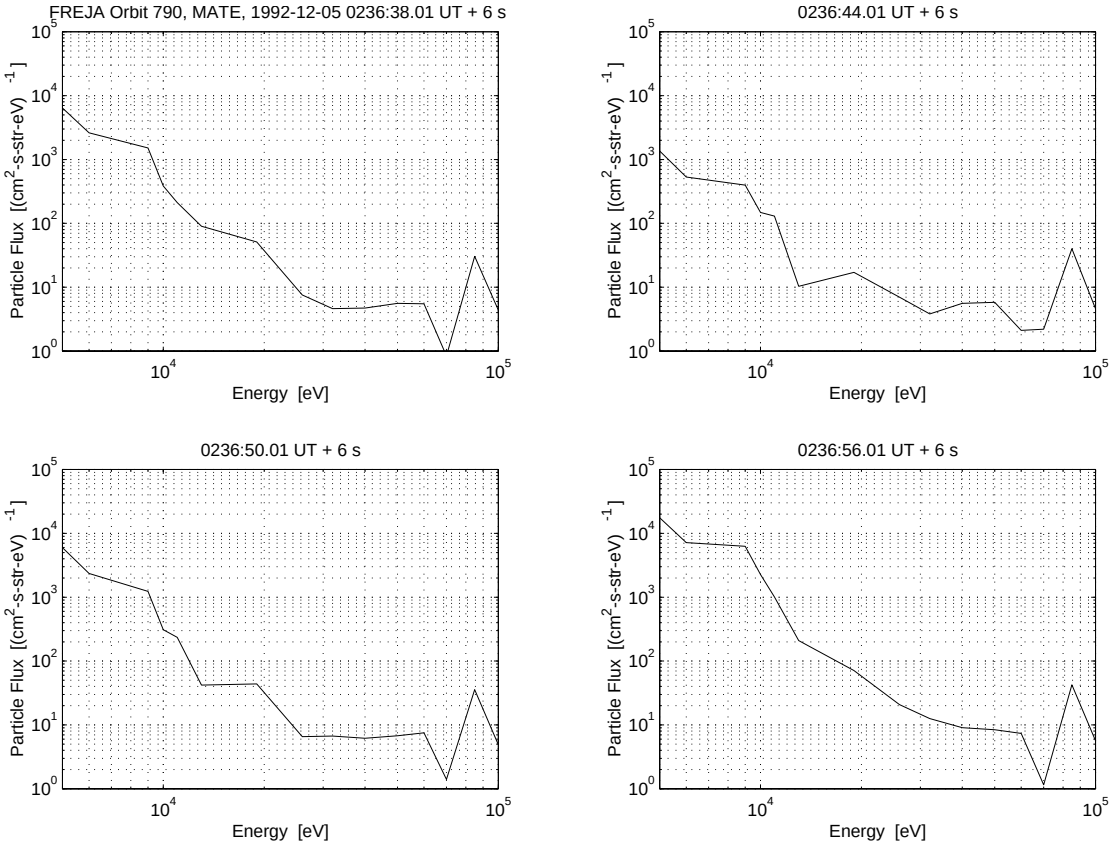

Figure 5.3.5a: MATE data. See Figure 5.3.4a.

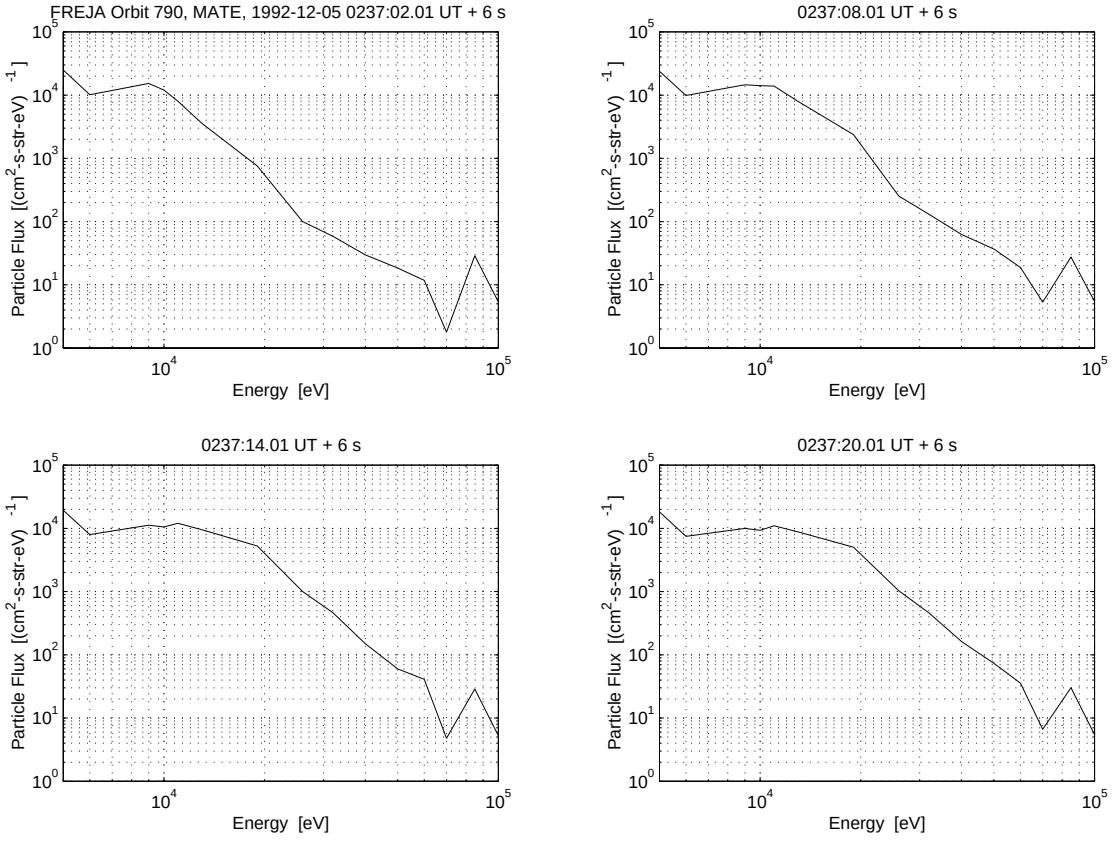

Figure 5.3.5b: MATE data. See Figure 5.3.4a.

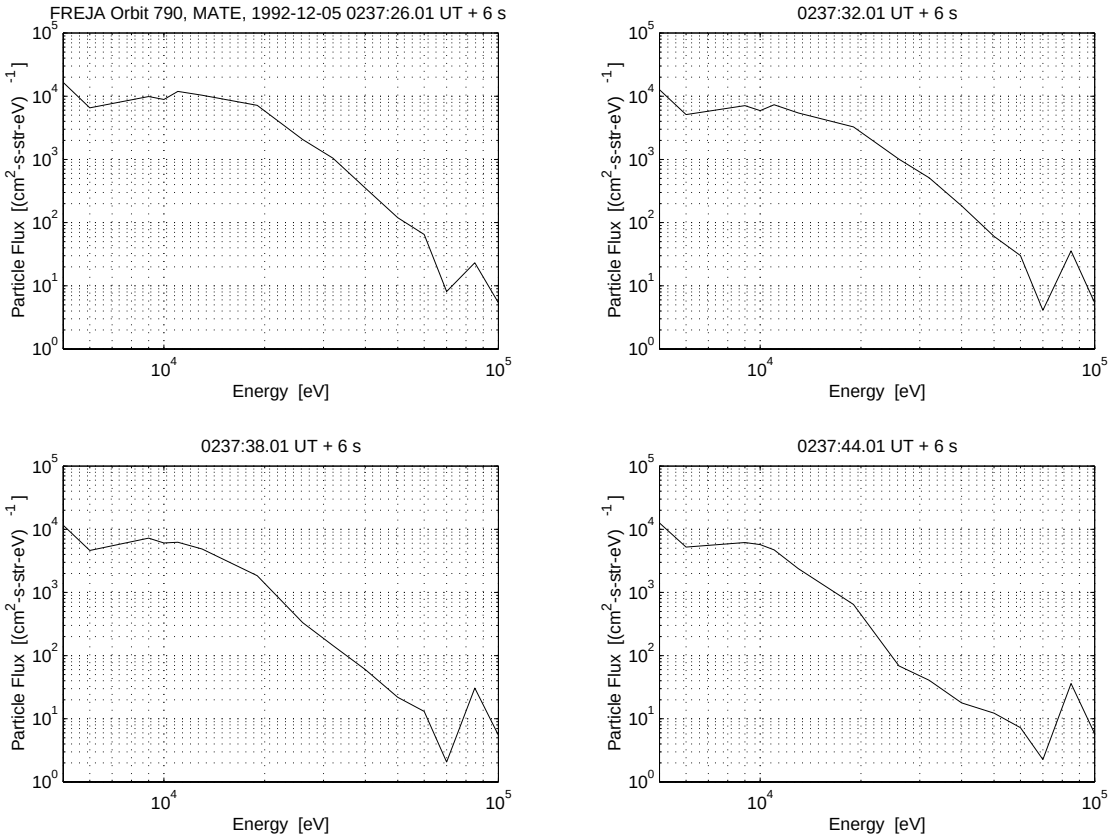

Figure 5.3.5c: MATE data. See Figure 5.3.4a.

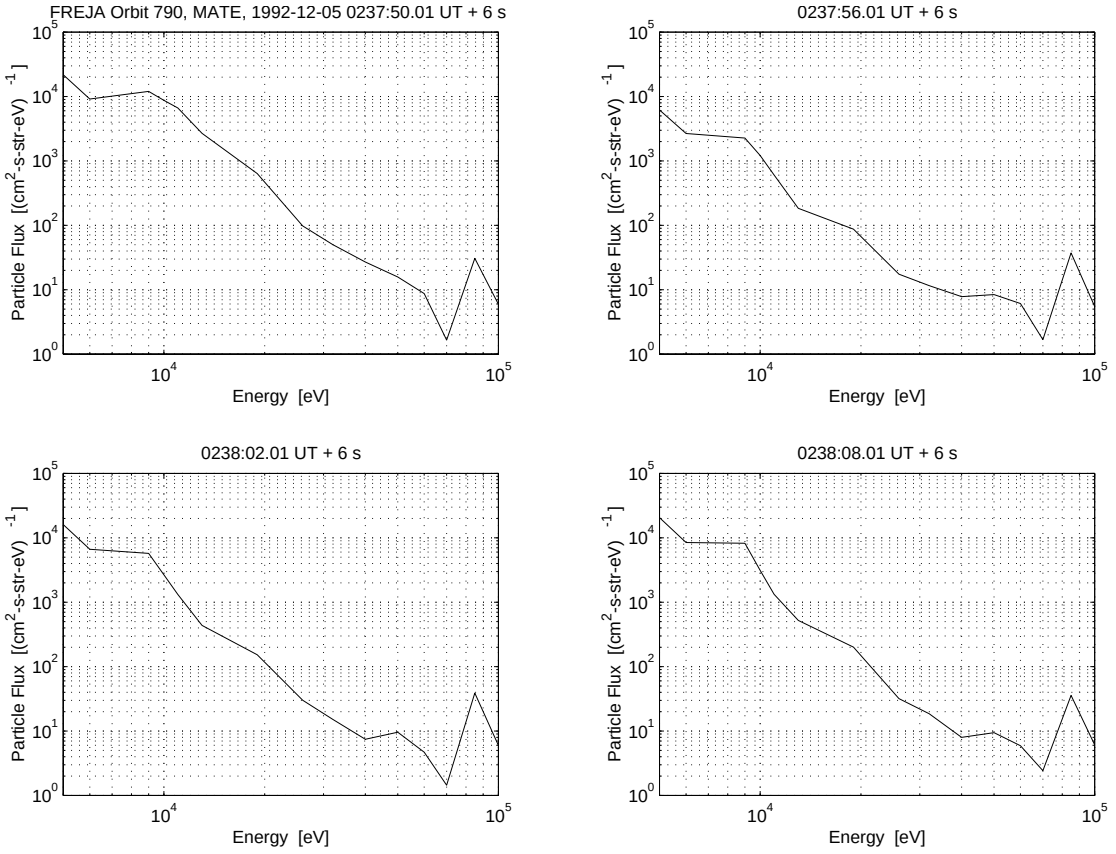

Figure 5.3.5d: MATE data. See Figure 5.3.4a.

Ion distributions around maximum charging are displayed in Figure 5.3.6a. They show the typical lifted-in-energy all-pitch-angle distribution of a charging event of about -65 V. Some indications of simultaneously occurring ion conics can be seen around 90° pitch-angle. For comparison, ion distributions from the ion conic event preceding the charging event, are presented in Figure 5.3.6b, where clear ion conics with energies up to 1.5 keV can be detected.

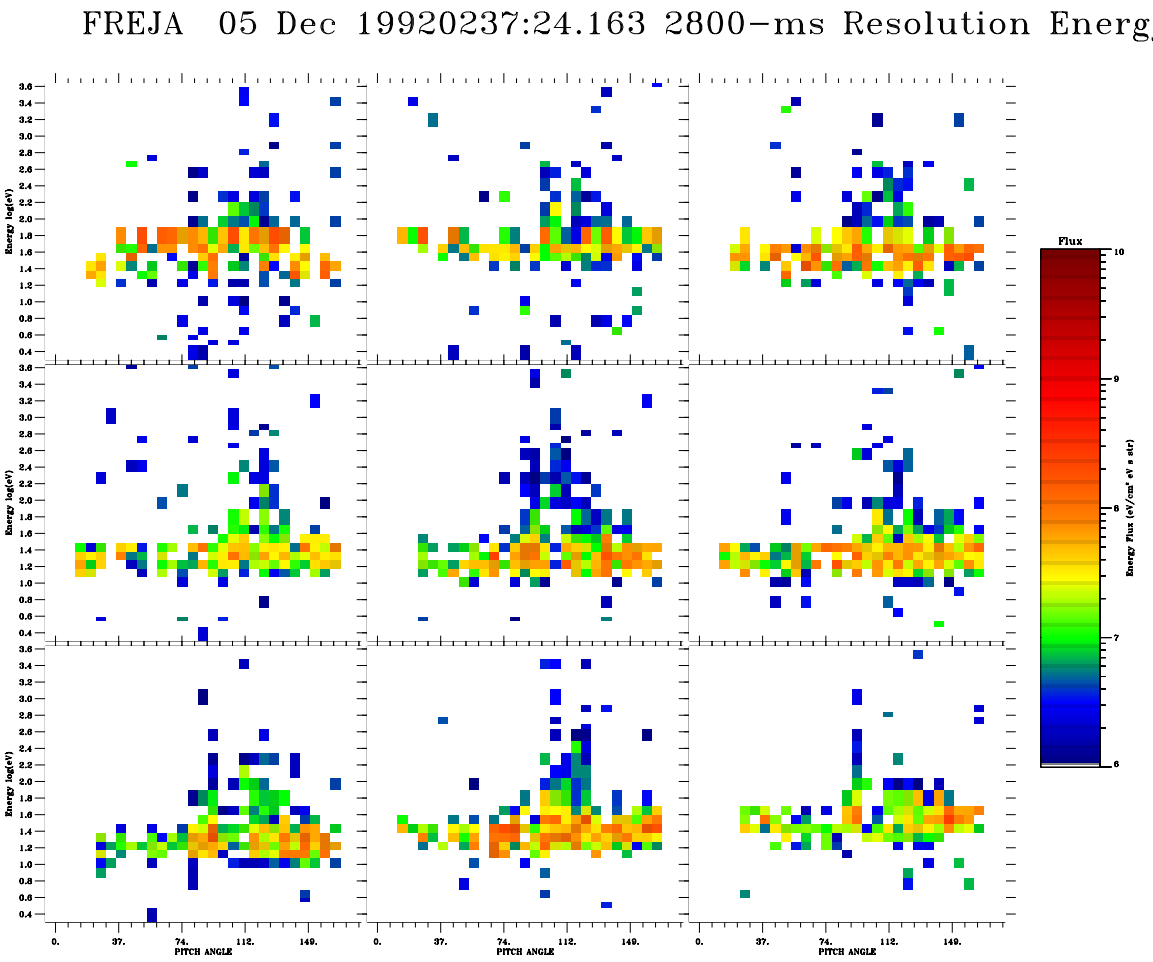

Figure 5.3.6a: The O^+ distributions during maximum charging (panel 2, -65 V).

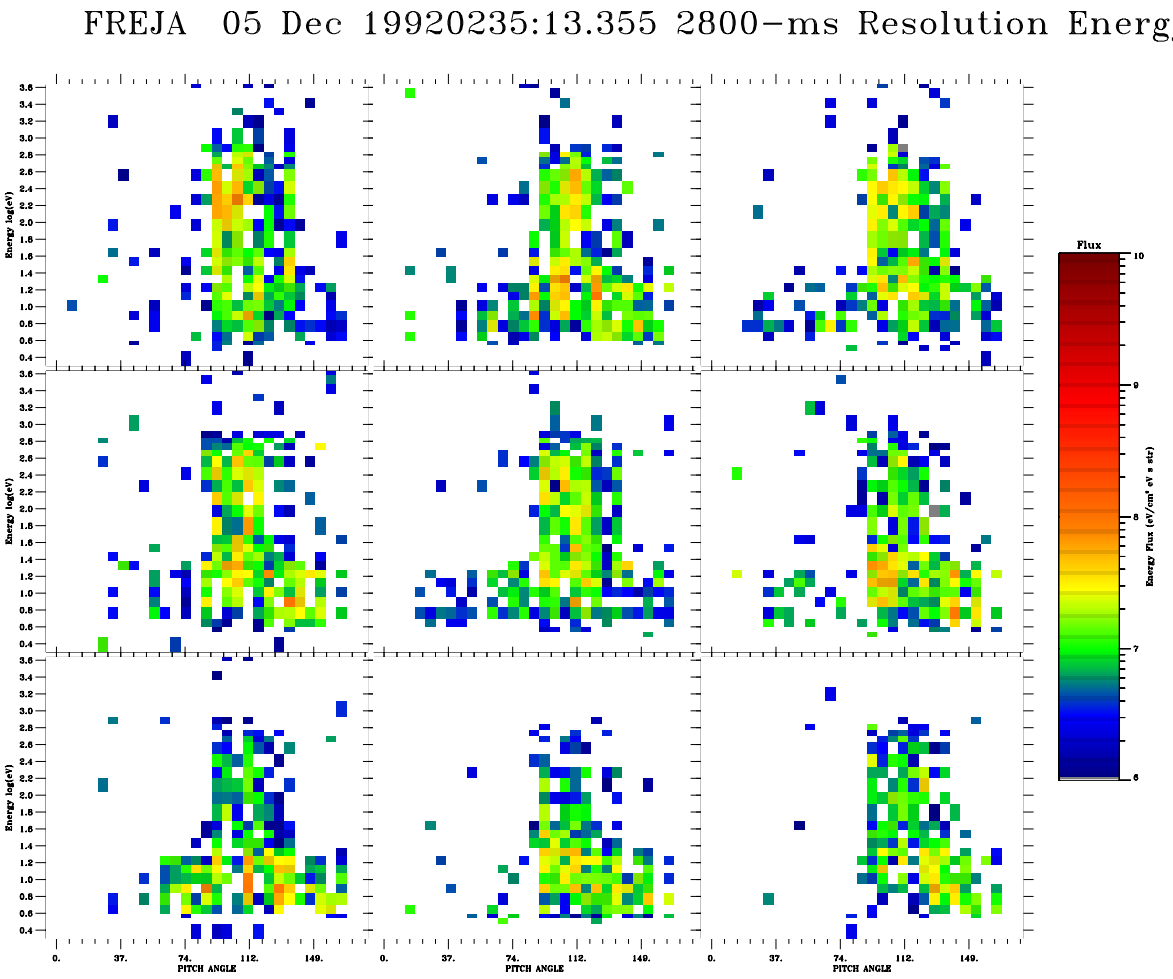

Figure 5.3.6b: Ion distributions from the ion conic event preceding the charging event. Ion conics with energies up to 1.5 keV can be detected.

Conclusions from orbit 790:

- The charging events started when the inverted-V electron energy peak reached above a few keV and the electron flux increased by an order of magnitude above these energies.
- Both electron peak energy and flux increased simultaneously, i.e. they were correlated.
- Spacecraft charging may occur during terminator conditions, i.e. when photoelectron emission from the spacecraft surface is expected to be significant. On the other hand, no charging was detected in the preceding full sunlight conditions despite heavy energetic electron precipitation associated with an auroral substorm.
- There are instrument disturbances due to the charging events in the Langmuir probe, MF and LF electric, and the TICS measurements

5.4 EVENT 4: ORBIT 1651 (TYPICAL CHARGING)

Overview Data, 93.02.08, Prince Albert

The overview data for the particle measurements are presented in Figure 5.4.1. The ions are lifted in energy between about 0558:00 - 0600:00 UT (panels 1-3) at the same time as enhanced fluxes of high energy electrons are detected (TESP, panel 7). The event occurs during eclipse (panel 4). The MATE measures only the integrated flux during this orbit.

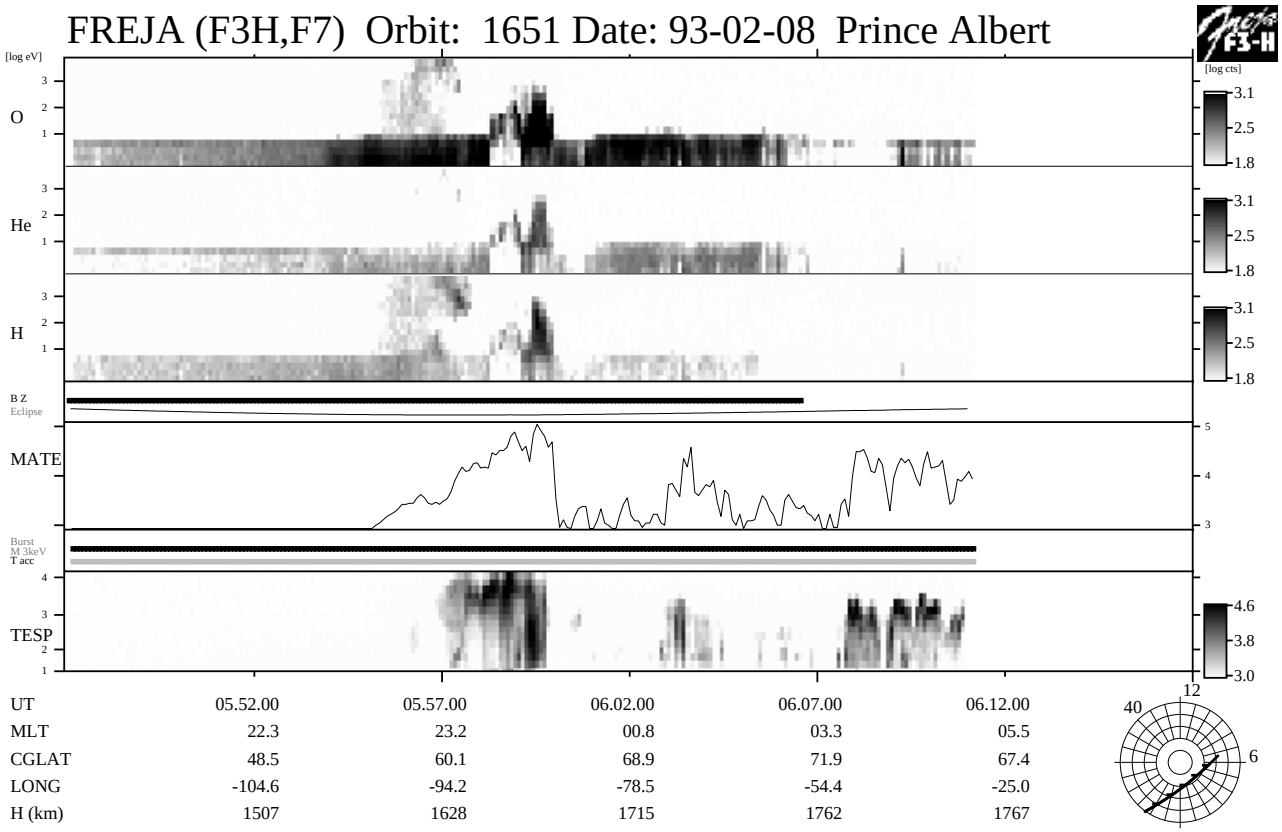

Figure 5.4.1: Overview particle data from orbit 1651. A typical charging event occurs during eclipse (panel 4) near 0558:30 UT just to be followed by a transverse ion heating event. A clear inverted-V structure (panel 7) can be seen in the TESP electron data when charging appears.

Figures 5.4.2 and 5.4.3 show a blow up of the particle and plasma wave data around the uplifted ion event in the interval 0558:10 - 0600:00 UT. After 0959:10 UT the ion energy increase is not accompanied with a clear dropout in the LP current, and is therefore likely to be due to ion heating rather than spacecraft charging. The HF narrow-band emission based estimates for the electron density correspond to densities inferred from the LP current, except for times of LP current dropout. The cold plasma density varies between $5 \cdot 10^8$ - $3 \cdot 10^9$ m^{-3}. Charging levels of a few tens of volts negative are inferred from the ion data, and the charging events are correlated with auroral inverted-V events with high energy electrons. Both the peak energy and the electron flux increase during charging times.

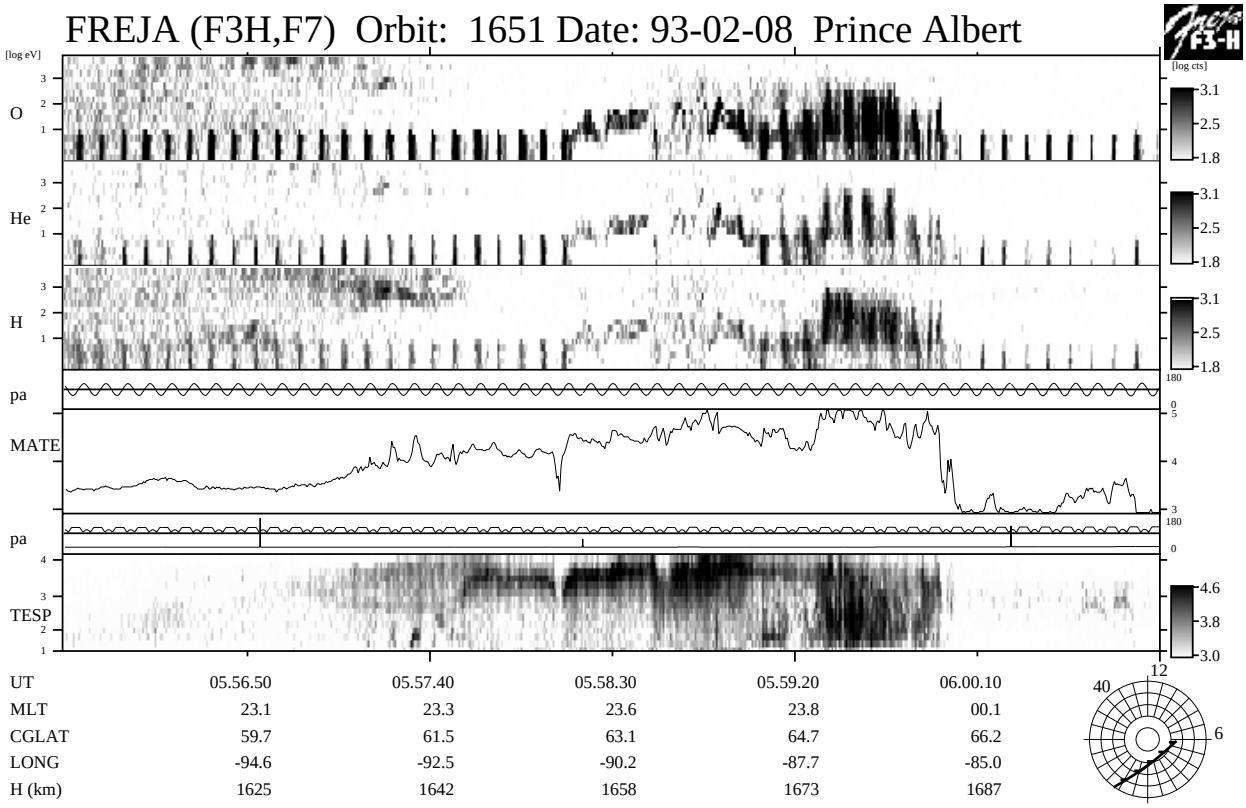

Figure 5.4.2: A blowup of Figure 5.4.1 around the charging event. Both the peak energy and electron flux increases during negative charging of Freja.

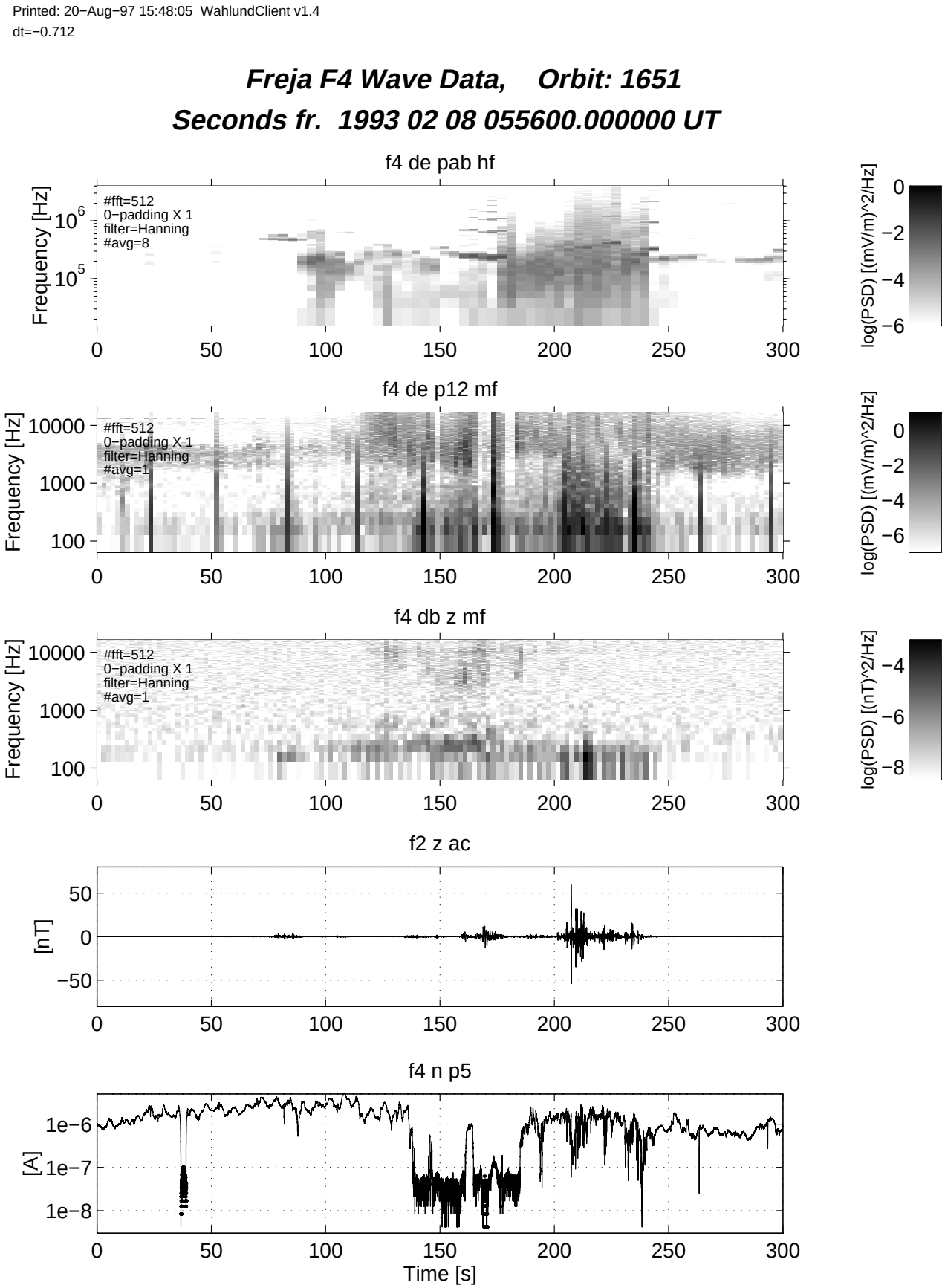

Figure 5.4.3: Plasma wave data corresponding to the particle data in Figure 5.4.2.

Detailed Particle Distributions

The TESP electron spectra during the charging event are shown in Figure 5.4.4. A typical inverted-V like electron spectrum with a clear energy peak near 7 keV can be seen in panel 2, which is replaced by a somewhat more energetic distribution in panel 3, to be relaxed in panel 4 (compare with panel 5 in Figure 5.4.2). The peak flux does not change significantly in panels 3 and 4. Instead an increased flux of lower energy electrons appears in panels 3 and 4, which may inhibit charging by producing an excess of secondary electrons. The detailed ion distributions are shown in Figure 5.4.5, where charging levels up to -40 V is inferred in panels 2 - 4.

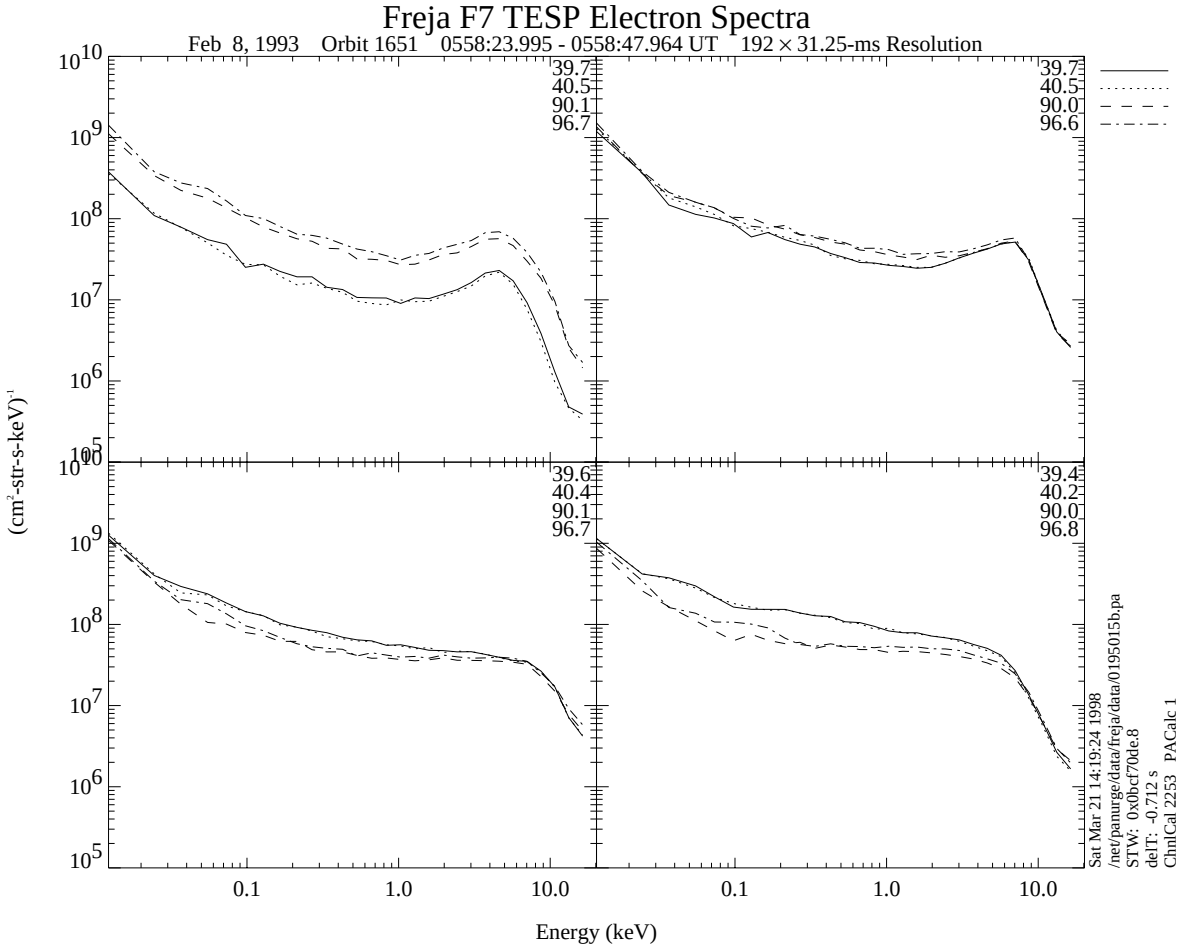

Figure 5.4.4: TESP electron spectra corresponding to the charging event displayed in Figure 5.4.2.

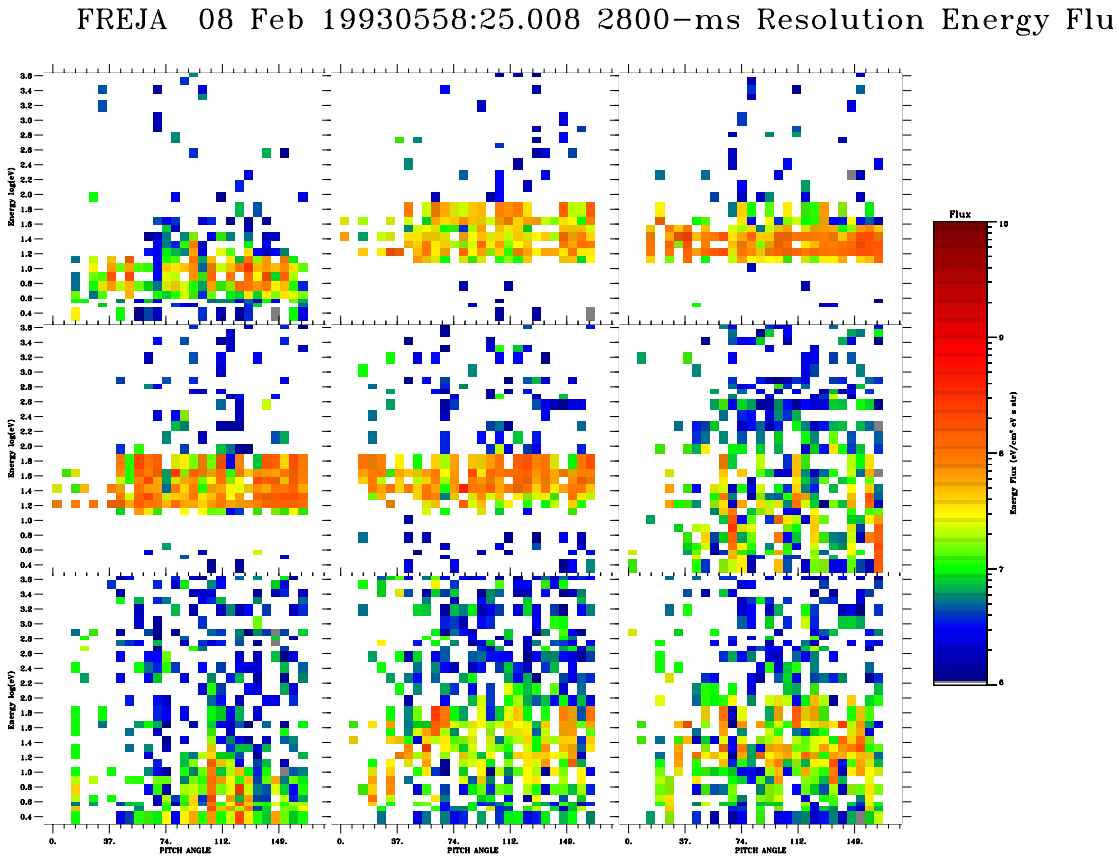

Figure 5.4.5: The O^+ distributions reveal negative charging of about -40 V in panels 2 to 4.

Conclusions from orbit 1651:

- both the inverted-V electron peak energy and flux increased during the charging event,
- an enhanced level of low energy (< 1 keV) electrons seemed to inhibit the charging,
- no sudden drop in plasma density seems to have occurred during the charging event,
- there are instrument disturbances due to the charging event in the Langmuir probe and the TICS measurements.

5.5 EVENT 5: ORBIT 5802 (CHARGING AND ION HEATING)

Overview Data, 93.12.19, Prince Albert

The overview data for the particle measurements from orbit 5802 are presented in Figure 5.5.1. The ions are lifted in energy between 0747:00 - 0752:00 UT (panels 1-3). However, only the first part of this period seems to be associated with enhanced fluxes of high energy electrons (panel 7), even though the information above 25 keV is unknown. The whole event occurs during eclipse (panel 4). The MATE measures only the integrated flux during this orbit.

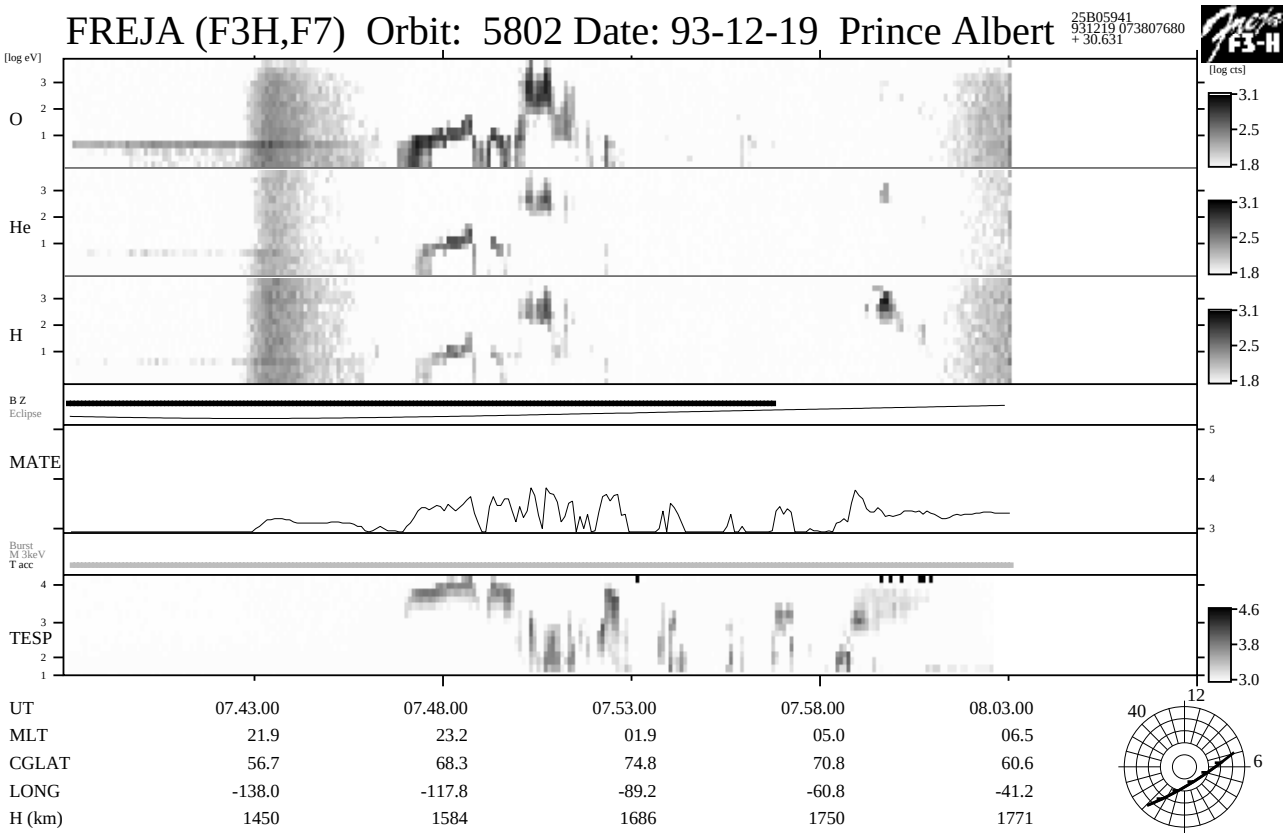

Figure 5.5.1: Overview particle data from orbit 5802. This orbit present two events with "uplifted" ion populations around 0748:00 UT and 0750:30 UT. Both events occur in eclipse. The first event is associated with energetic inverted-V type electrons, the other with lower energy so called field-aligned suprathermal electron bursts. The first event is a charging event, the following is an auroral transverse energization event.

Figures 5.5.2 and 5.5.3 show a blow up of the particle and plasma wave data around the uplifted ion event, which can be divided into three regions (0747:00 - 0750:00 UT, 0750:00 - 0751:30 UT, and the event after 0752:00 UT, Figure 5.5.2, panels 1-3). The events in the first part are associated with dropouts in the CYLP current, when the HF emissions still indicate large plasma densities of $2\text{-}8 \cdot 10^8$ m^{-3}. The middle event period shows very low densities below $7 \cdot 10^7$ m^{-3} according to the HF emissions and the CYLP current dropouts are not completely in the bottom. Also, there are no enhanced high energy electron fluxes associated with this event. Rather the TESP data show evidence for suprathermal electron bursts with energies below a few hundred eV. The third event

after 0752:00 UT is associated with both high energy electrons and CYLP current dropouts, but there is no detectable uplift in ion energies. We interpret these data as follows; the event in the first period are due to spacecraft charging, the event in the middle period is due to ion heating, and the last event is also a charging event, but with fast intermittent fluctuations of low level charging not readily detectable by the TICS instrument. In the first event the charging starts when the inverted-V peak energy approaches 10 keV, while no charging occurrs if the inverted-V peak energy is below about 5 keV. Thus, a threshold energy for charging seems to be present also for this charging event, which can be due to in the crossover secondary emission yield energy of the Freja surface materials.

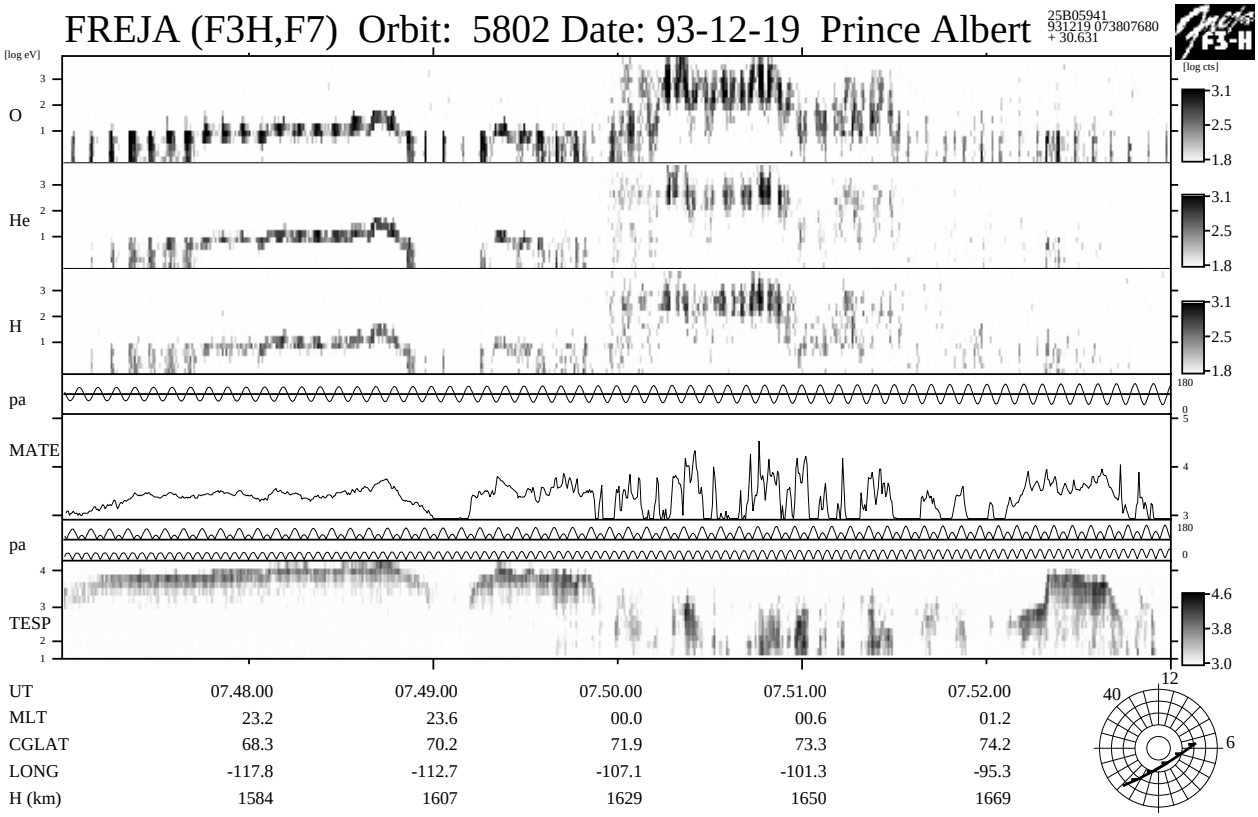

Figure 5.5.2: A blow up of Figure 5.5.1, showing the clear charging event with its associated high energy inverted-V electrons and the transverse ion heating event with its associated suprathermal electron bursts.

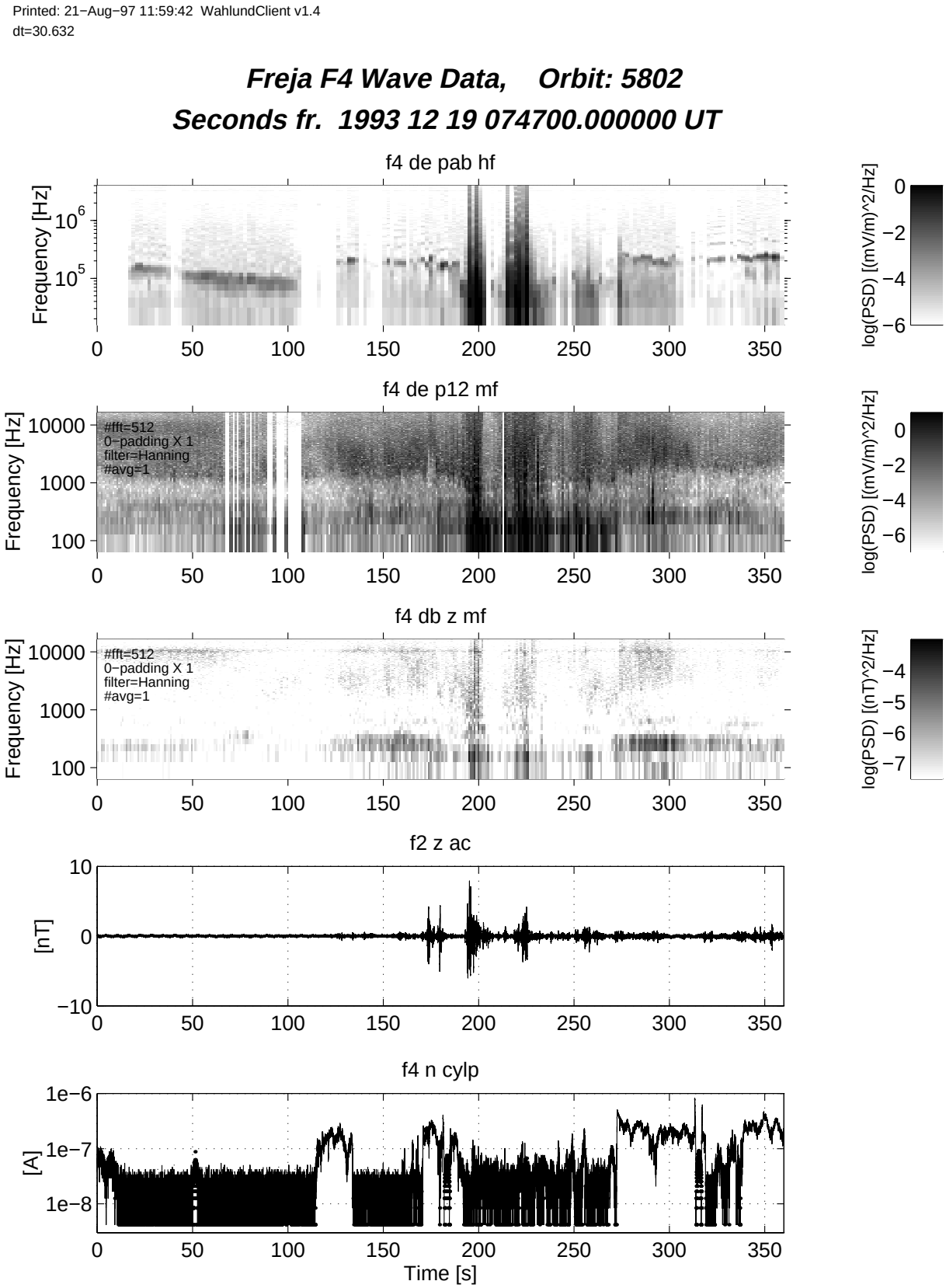

Figure 5.5.3: Plasma wave data corresponding to the particle data in Figure 5.5.2. The density is very low during the transverse ion heating event and the HF emissions correspond well with the low LP currents during that time (+190 s - +270 s). On the other hand, they do not correspond well during the charging events before +170 s.

Detailed Particle Distributions

Figure 5.5.4a and 5.5.5a display the TESP electron spectra and TICS ion distributions for the first charging event near 0748:20 UT. A clear inverted-V electron energy peak near 10 keV can be detected together with uplifted energy distributions of the ions at all pitch-angles. Negative charging levels reaching -12 V are inferred from the ion data.

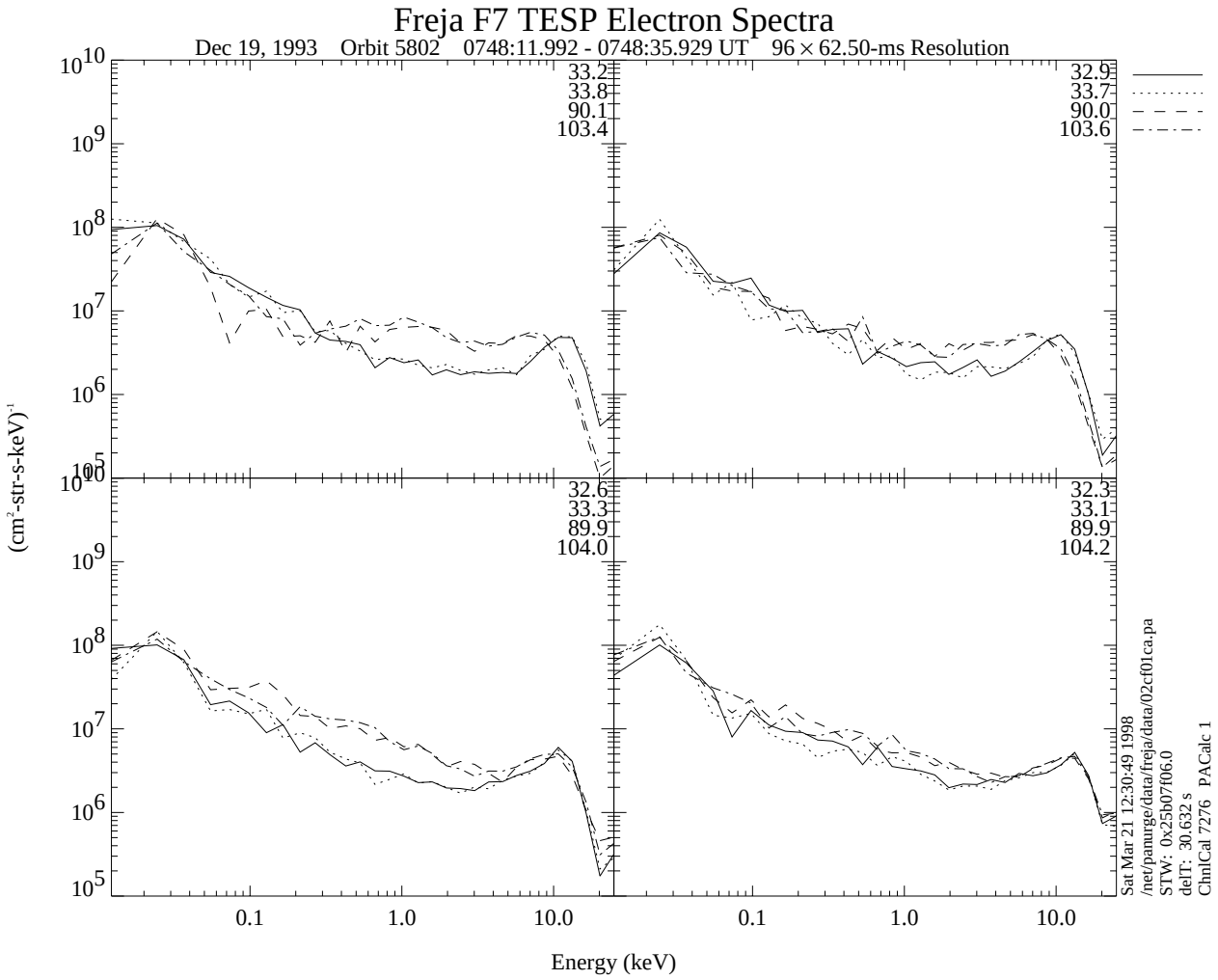

Figure 5.5.4a: TESP electron data from the charging period of this orbit. Auroral inverted-V electron peaks reach 10 keV during charging.

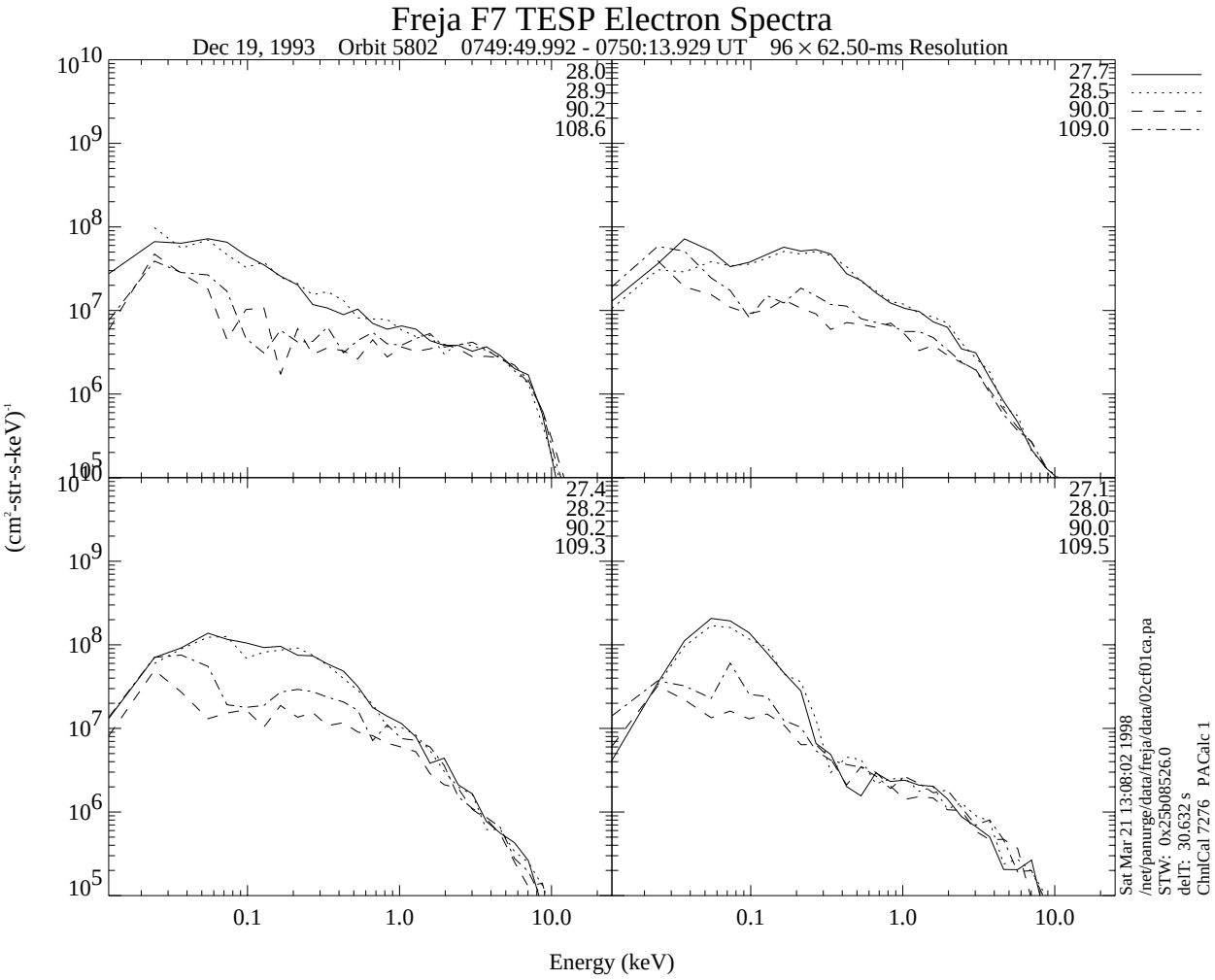

Figure 5.5.4b: TESP electron data from the ion conic period. Intense rather field-aligned low energy (< 1 keV) fluxes are detected.

Detailed TESP electron spectra and TICS ion distributions from the start of the ion conic event are presented in Figures 5.5.4b - 5.5.4c and 5.5.5b respectively. The electron spectra show no trace of high energy inverted-V electrons. Instead rather field-aligned distributed suprathermal electron bursts can be detected at energies below a couple of keV. The corresponding ion distributions evolves from a ram-distribution (panel 1) to an energetic ion conic (panels 2 - 7), which suddenly is lifted to about 250 eV (panels 8 - 9) most probably due to transverse ion heating in connection with the mirror force produced by Earth's diverging magnetic field.

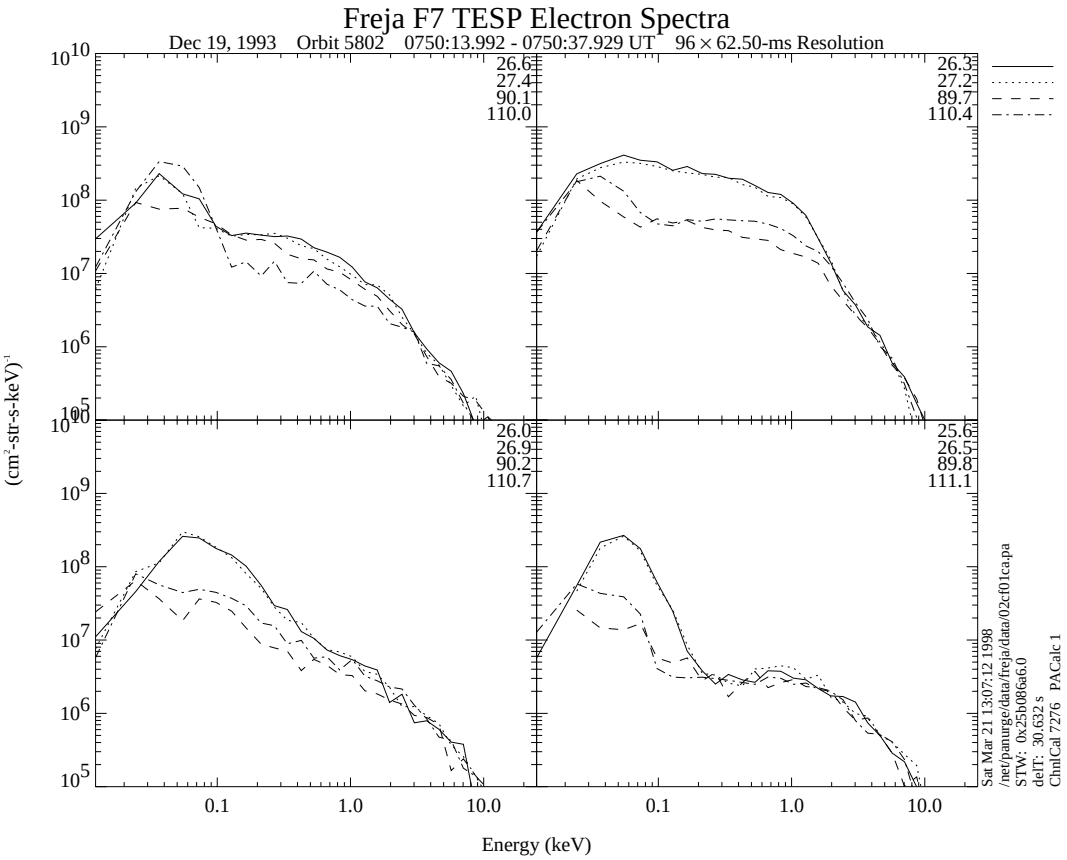

Figure 5.5.4c: TESP electron data. Continuation of Figure 5.5.4b.

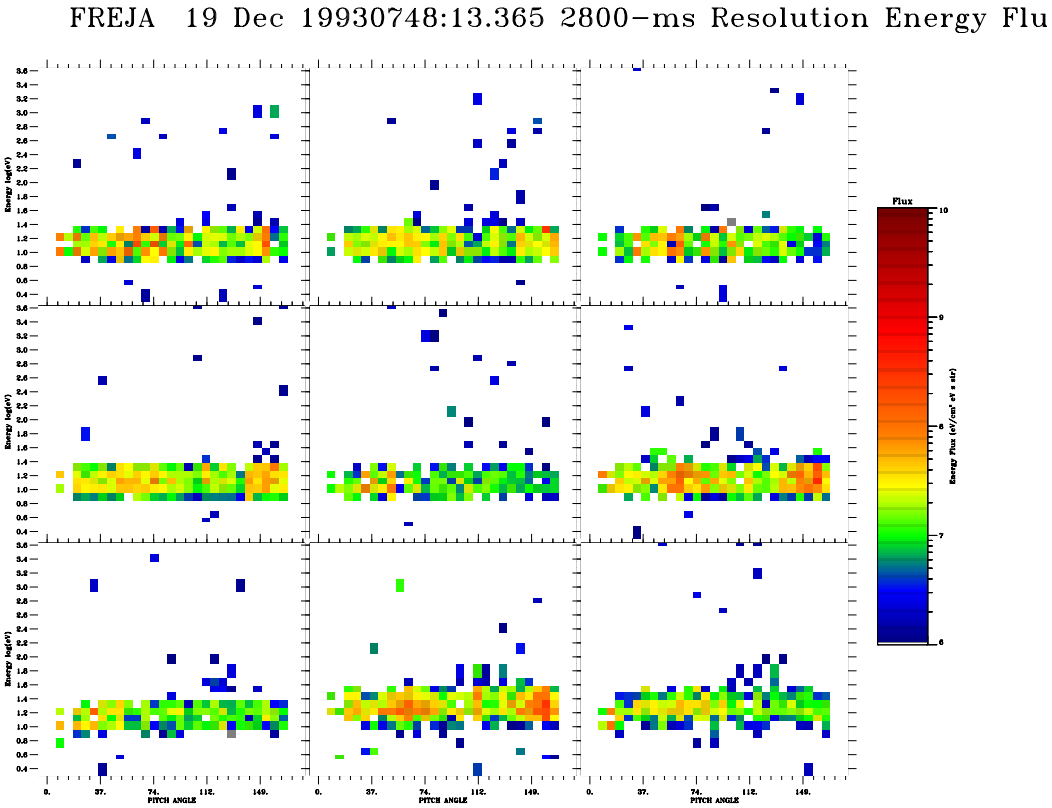

Figure 5.5.5a: The O^+ distribution functions show low level charging of about -12 V.

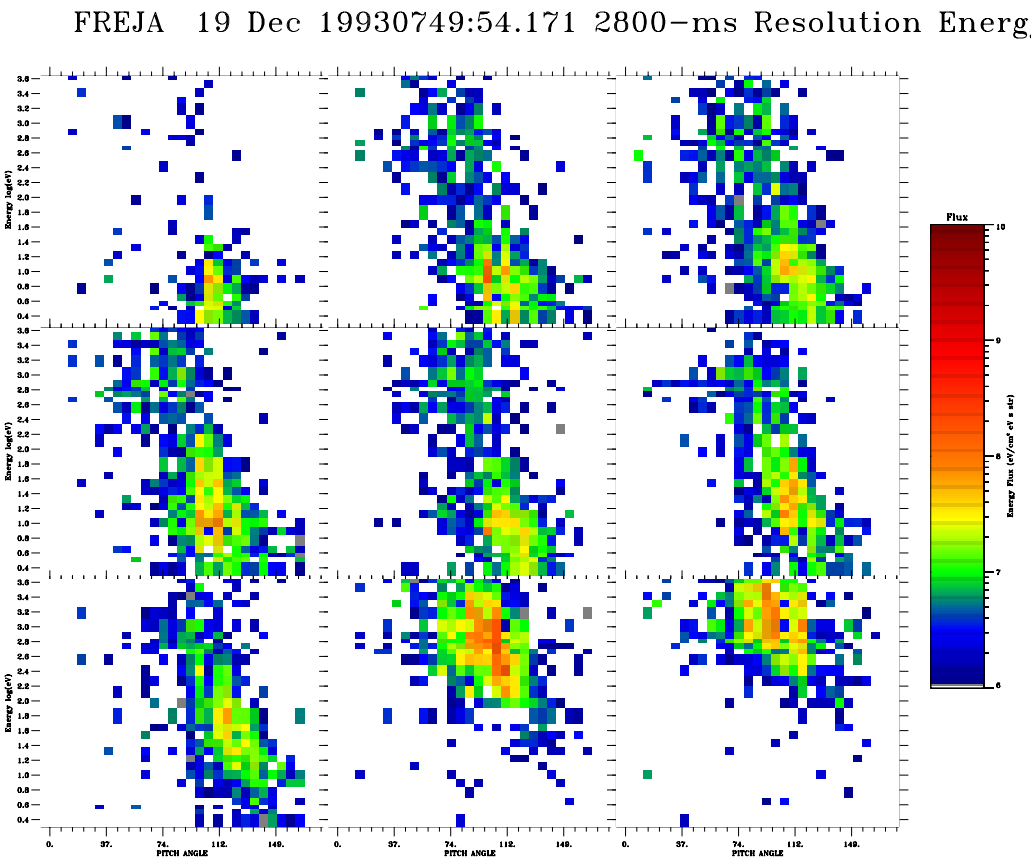

Figure 5.5.5b: These O^+ distribution functions show a nice transition from the spacecraft ram flow signature (panel 1), the transverse energization of the oxygen ions (panels 2 - 6), which in the end of this measurement sequence show the whole ion population accelerated upwards most probably by the action of the magnetic mirror force (panels 7 - 9).

Conclusions from orbit 5802:

- The inverted-V peak energy reached above about 5 keV during the charging events, while no charging was detected when this energy peak fell below 5 keV.
- Transverse ion heating may produce uplifted ion events similar to those during spacecraft charging. However, the detailed ion energy pitch-angle distributions during these two cases are considerably different and can easily be distinguished if accurate analysis is made. Also, transverse ion heating in the Freja data set is most often associated with field-aligned suprathermal electron bursts rather than isotropic inverted-V precipitation.
- There are instrument disturbances due to the charging events in the Langmuir probe, MF and LF electric, and the TICS measurements.